THE JOURNAL OF PHYSICAL CHEMISTRY B

Article

pubs.acs.org/JPCB

# Interaction of Charged Colloidal Particles at the Air−Water Interface

Matheus Girotto, Alexandre P. dos Santos, and Yan Levin*

Instituto de Física, Universidade Federal do Rio Grande do Sul, Caixa Postal 15051, CEP 91501-970, Porto Alegre, RS, Brazil

**ABSTRACT:** We study, using Monte Carlo simulations, the interaction between charged colloidal particles confined to the air−water interface. The dependence of force on ionic strength and counterion valence is explored. For 1:1 electrolyte, we find that the electrostatic interaction at the interface is very close to the one observed in the bulk. On the other hand, for salts with multivalent counterions, an interface produces an enhanced attraction between like charged colloids. Finally, we explore the effect of induced surface charge at the air−water interface on the interaction between colloidal particles.

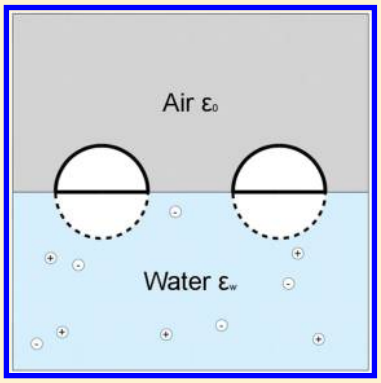


## INTRODUCTION

The presence of colloidal particles at a fluid−fluid interface can significantly lower the interfacial energy, giving them an amphiphilic character. The adsorption energies can be many thousands of $k_BT$'s even for relatively small colloidal particles of only a few hundred angstroms, making the colloidal adsorption an irreversible process.[1] To help the dispersion in water, colloidal particles are often synthesized with ionic groups at their surface. When in water, these groups dissociate, leading to an effective surface charge which helps to stabilize a suspension against flocculation and precipitation. The dissociation of surface groups is favored by the entropic gain of the release of counterions, and is opposed by the electrostatic self-energy penalty. Adsorption of charged colloidal particles to the air−water interface prevents the dissociation of charged groups exposed to the low dielectric environment, since this leads to a very large electrostatic free energy penalty.

Colloidal particles confined to an electrolyte−air interface exhibit many interesting properties which have stimulated a number of theoretical and experimental works.[2−15] The first direct observation of colloidal bidimensional structure was made by Pieranski more than 3 decades ago.[16] Pieranski showed that the asymptotic electrostatic potential between two colloidal particles, confined to an interface, decays as $1/r^3$. This repulsive potential has a suggestive dipole−dipole-like form, which results in the formation of a two-dimensional triangular lattice by the adsorbed colloidal particles. Using linearized Poisson−Boltzmann (PB) theory, Hurd calculated the interaction potential between two point-particles confined to the air−electrolyte solution[1] interface. The interaction potential for large separations was found to have precisely a dipole−dipole-like form observed in Pieranski's experiments.[1,17−21]

Hurd's calculations based on the linearized PB equation are sufficient to study the interaction potential at large separations for suspensions in a symmetric 1:1 electrolyte. However, at short separations, when the electrostatic potential is large, linearization of the PB equation cannot be justified. This requires a complicated numerical solution or some form of Derjaguin-like approximation based on the nonlinear solution of the PB equation in a planar geometry. The situation becomes even more complicated if the suspension contains multivalent counterions, in which case strong electrostatic correlations completely invalidate the use of PB theory.[22] In this paper, we will explore the interaction between two colloidal particles confined to a dielectric air−electrolyte interface using Monte Carlo (MC) simulations. In this respect, our work should provide a benchmark against which future analytical and numerical approximations can be tested. The system studied is depicted in Figure 1. In the next section, we will present our model and discuss the MC method used to perform the simulations.

## MODEL AND MONTE CARLO SIMULATIONS

There are a number of different techniques developed in the literature which can be used to simulate systems with long-range interactions. The difficulty of studying these systems is that there is no characteristic distance at which the interaction potential can be cut off. This prevents us from using the usual periodic boundary conditions. Instead, to explore the thermodynamic limit, one must create an infinite set of periodic replicas of the system. The particles then interact not only with the other particles of the simulation cell but also with the images in all of the replicas. To efficiently sum over the replicas, one can use a 3D Ewald summation[23] method. This technique is well suited to study bulk suspensions. Unfortunately, it is not appropriate to study interfacial geometry in

**Special Issue:** William M. Gelbart Festschrift

**Received:** October 15, 2015
**Revised:** November 6, 2015
**Published:** November 9, 2015





DOI: 10.1021/acs.jpcb.5b10105
J. Phys. Chem. B 2016, 120, 5817−5822

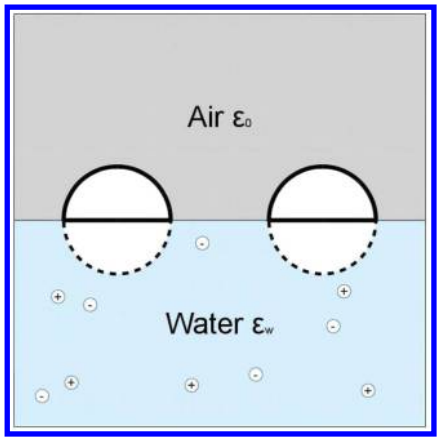


**Figure 1.** Colloidal particles at an air−electrolyte solution interface. Only the colloidal hemisphere which is hydrated is charged.

which a system should be replicated only in two out of three dimensions. To overcome this difficulty, there have been developed a number of simulation algorithms specifically adopted to the slab geometry.[24−32] The 2D Ewald summation method developed by Leeuw and Perram[24] is the most accurate but is computationally very expensive.[25,31,32] A way to overcome the limitations of 2D Ewald summation is to use a 3D Ewald summation technique with an asymmetric simulation cell. The aperiodic dimension of this cell must be made to include a sufficiently large empty region, free of any charged particles. In this way, the particles in the replicas in the aperiodic dimension (lets call it the $z$ direction) will interact very weakly across the empty region.[33] In order to use this technique, a surface term must be added to the total energy of the system,[34,35] to account for the conditional convergence of the sum over the replicas. This term depends on the geometry of the system, the total electric dipole moment in the $z$ direction, and the dielectric constant of the surrounding medium.[23,36−39]

Our simulation cell has the volume $V = L^3$, with $L = 200$ Å. The electrolyte is confined in the region $-L/2 < x < L/2$, $-L/2 < y < L/2$, $-L/2 < z < 0$, and air, in $0 < z < L/2$. Water is treated as a continuum of dielectric constant $\varepsilon_w = 80\varepsilon_0$, where $\varepsilon_0$ is the dielectric constant of a vacuum. The Bjerrum length, defined as $\lambda_B = q^2/\varepsilon_w k_B T$, is 7.2 Å, where $q$ is the proton charge. This value is appropriate for water at room temperature. The adsorbed colloidal particles have radius of 20 Å and charge of $Z = -20q$ or $Z = -30q$, distributed uniformly over the hemisphere that is hydrated. This surface charge density corresponds to $\sigma \approx -0.13\ C/m^2$, close to experimental values. The hemispheres exposed to the low dielectric environment remain uncharged. The salt concentration is varied between 25 and 125 mM, in order to explore its influence on the interaction between the colloidal particles. The effect of counterion valence is explored by changing between 1:1, 2:1, and 3:1 electrolyte. The radius of all monovalent ions is set to 2 Å, and that of multivalent counterions, to 3 Å. To account for colloidal surface charge, we place 98 uniformly spaced point charges—each of charge $Z/98$—along the surface.

The total electrostatic energy of a charge neutral system containing $N$ ions of charges $q_i$, in aqueous medium, near a dielectric interface was calculated in refs 40 and 41. To efficiently sum over all the replicas, the electrostatic potential is split into long-range and short-range contributions. The electrostatic energy can then be written as

$$U = U_S + U_L + U_{self} + U_{cor} \tag{1}$$

The short-range electrostatic energy is $U_S = (1/2)\sum_{i=1}^{N} q_i \phi_i^S(\mathbf{r}_i)$, where $\phi_i^S(\mathbf{r})$ is

$$\phi_i^S(\mathbf{r}) = {\sum_{j=1}^{N}}' q_j \frac{\mathrm{erfc}(\kappa_e|\mathbf{r} - \mathbf{r}_j|)}{\varepsilon_w|\mathbf{r} - \mathbf{r}_j|} + \sum_{j=1}^{N} \gamma q_j \frac{\mathrm{erfc}(\kappa_e|\mathbf{r} - \mathbf{r}'_j|)}{\varepsilon_w|\mathbf{r} - \mathbf{r}'_j|} \tag{2}$$

where $\mathbf{r}_j$ is the position of charge $q_j$ and $\mathbf{r}'_j = \mathbf{r}_j - 2z_j\hat{\mathbf{z}}$ is the position of the image charge $\gamma q_j$. The prime on the summation means that $j \neq i$. The dumping parameter $\kappa_e$ is set to $\kappa_e = 4/L$, while $\gamma = (\varepsilon_w - \varepsilon_a)/(\varepsilon_w + \varepsilon_a)$; $\varepsilon_w$ and $\varepsilon_a$ are the dielectric constants of water and the dielectric material, respectively. The self-energy contribution is

$$U_{self} = -\frac{\kappa_e}{\varepsilon_w\sqrt{\pi}} \sum_{i=1}^{N} q_i^2 \tag{3}$$

The long-range electrostatic energy is

$$U_L = \sum_{\mathbf{k}} \frac{2\pi}{\varepsilon_w V|\mathbf{k}|^2} \exp\left(-\frac{|\mathbf{k}|^2}{4\kappa_e^2}\right)[A(\mathbf{k})^2 + B(\mathbf{k})^2 + A(\mathbf{k})C(\mathbf{k}) + B(\mathbf{k})D(\mathbf{k})] \tag{4}$$

where

$$A(\mathbf{k}) = \sum_{i=1}^{N} q_i \cos(\mathbf{k}\cdot\mathbf{r}_i)$$

$$B(\mathbf{k}) = -\sum_{i=1}^{N} q_i \sin(\mathbf{k}\cdot\mathbf{r}_i)$$

$$C(\mathbf{k}) = \sum_{i=1}^{N} \gamma q_i \cos(\mathbf{k}\cdot\mathbf{r}'_i)$$

$$D(\mathbf{k}) = -\sum_{i=1}^{N} \gamma q_i \sin(\mathbf{k}\cdot\mathbf{r}'_i)$$

These functions are easily updated for each new configuration in a MC simulation. The number of vectors $\mathbf{k}$'s defined as $\mathbf{k} = (2\pi n_x/L, 2\pi n_y/L, 2\pi n_z/L)$, where $n$'s are integers, is set to around 700 in order to achieve fast convergence. Yeh and Berkowitz[35] found that the regular 3D Ewald summation method with an energy correction can reproduce the same results as the 2D Ewald summation method, with a significant gain in performance. Taking into account the dielectric discontinuity and the induced image charges, the energy correction for the slab geometry is

$$U_{cor} = \frac{2\pi}{\varepsilon_w V} M_z^2 (1 - \gamma) \tag{5}$$

where $M_z = \sum_{i=1}^{N} q_i z_i$ is the total electric dipolar momentum in the $\hat{z}$ direction.[40]

To perform MC simulations, we use the regular Metropolis algorithm with $10^5$ MC steps to achieve equilibrium, while the force averages are performed with $10^5$ uncorrelated samples, each sample obtained at an interval of 100 movements per particle, after the equilibrium has been achieved. During the equilibration, we adjusted the length of the particle displacement to achieve an acceptance of trial moves near 50%. We then calculate the force between two colloidal particles confined to an interface. The total force contains both



DOI: 10.1021/acs.jpcb.5b10105
J. Phys. Chem. B 2016, 120, 5817−5822

electrostatic and entropic contributions. To calculate the mean electrostatic force, we use the method of virtual displacement in which one of the colloidal particles is moved while the other colloidal particle and all the ions remain fixed, which implies that

$$\langle \mathbf{F}_{el} \rangle = \sum_i \langle -\nabla_{\mathbf{r}_i} U(\mathbf{r}_1, ..., \mathbf{r}_N) \rangle \tag{6}$$

In the above expression, the sum runs over the point particles which make up the colloidal surface charge.

The entropic force that arises from the transfer of momentum during the collisions between colloidal particles and ions can be calculated using the method introduced by Wu et al.[42] It consists of performing a small virtual displacement of colloidal particles along the line joining their centers—while all the microions remain fixed—and counting the number of resulting virtual overlaps between the colloidal particles and microions. The entropic force can then be expressed as

$$\beta F_{en} = \frac{\langle N^c \rangle - \langle N^f \rangle}{2\Delta R} \tag{7}$$

where $N^c$ is the number of virtual overlaps between the colloidal particles with the microions after a small displacement $\Delta R$ = 0.9 Å that brings colloidal particles closer together (superscript c stands for closer) and $N^f$ is the number of overlaps of colloidal particles with the microions after a displacement $\Delta R$ that moves the two colloidal particles farther apart (superscript f stands for farther).[43]

## RESULTS

We start by studying the dependence of the force between two colloidal particles trapped at the air−water interface on the concentration of 1:1 electrolyte. We first neglect the dielectric discontinuity across the interface by setting the dielectric constant of air to $\varepsilon_a = \varepsilon_w$, so that $\gamma = 0$. Later on, we will explore the effect of the surface charge induced at the dielectric air−water interface by the microions and colloids, by including image charges in the calculation of the total force. In this case, we will set the dielectric constant of air to $\varepsilon_a = \varepsilon_0$, resulting in $\gamma \approx 0.975$. In the present paper, we will neglect the image charges induced inside the colloidal particles[44,45]—this is equivalent to making the two hemispheres of colloidal particles exposed to air and water be composed of "air-like" and "water-like" dielectric materials, respectively. In Figure 2, we plot the force vs distance curve for three different salt concentrations.

As expected, when the concentration of 1:1 electrolyte increases, the force between colloidal particles decreases. This result is the same as that for colloids in the bulk electrolyte[22] which are well described by the DLVO theory.

We can now see if the force between two colloidal particles at an interface can also be described by the DLVO expression[22]

$$F = \frac{(Z_{eff})^2 \theta^2(\kappa a)}{\varepsilon_w} e^{-\kappa r} \left( \frac{\kappa}{r} + \frac{1}{r^2} \right) \tag{8}$$

where $Z_{eff}$ is the colloidal effective charge, $a$ is the colloidal radius, $\kappa = \sqrt{8\pi\lambda_B \rho_S}$ is the inverse Debye length, $\rho_S$ is the salt concentration, $r$ is the separation distance between particles, and $\theta(x)$ is a function given by

$$\theta(x) = \frac{e^x}{1 + x} \tag{9}$$

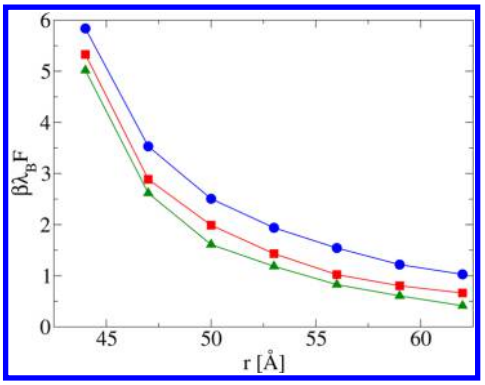


**Figure 2.** Force between two colloidal particles trapped at the air−water interface, for various 1:1 salt concentrations. Circles represent simulations with a 25 mM ($\kappa$ = 0.05 Å$^{-1}$) concentration of salt, squares with 75 mM ($\kappa$ = 0.09 Å$^{-1}$), and triangles with 125 mM ($\kappa$ = 0.12 Å$^{-1}$) of salt. The lines are guides to the eyes. Image effects are neglected.

Figure 3 shows that it is possible to account for the MC data using DLVO theory if the effective charge $Z_{eff}$ is adjusted to $Z_{eff}$

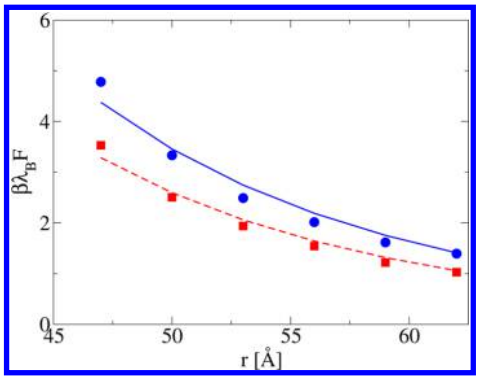


**Figure 3.** Force between two colloidal particles trapped at the air−water interface. Lines are the result of the DLVO theory with adjusted effective charge, while symbols represent MC simulations. Circles are for colloidal charge −30$q$, while squares are for charge −20$q$. This charge is distributed uniformly over the hydrated hemisphere. The monovalent salt concentration is 25 mM ($\kappa$ = 0.05 Å$^{-1}$). Image charges are not included.

$\approx -15.6q$ for colloidal particles of bare charge $Z = -20q$ and $Z_{eff} \approx -18q$ for colloidal particles with bare charge $Z = -30q$. Surprisingly, these effective charges are very close to the effective charge of colloidal particles in the bulk which can be calculated using Alexander's prescription:[46,47] $Z_{eff} \approx -15.9q$ and $Z_{eff} \approx -19.8q$ for colloids with bare charge $Z = -20q$ and $Z = -30q$, respectively. This agreement is quite surprising considering that for colloidal particles at the interface the charge is distributed only over the hydrated hemisphere, while for bulk colloids the *same* total charge $Z$ is uniformly distributed over the whole surface. In Figure 4, we present an explicit comparison of the interaction force obtained using MC simulations for two colloidal particles confined to an interface and two colloidal particles inside a bulk 1:1 electrolyte; see Figure 5. The bare charges of colloidal particles of both systems are the same. The two forces are practically identical; see Figure 4.

The agreement between interfacial and bulk forces does not extend to 2:1 and 3:1 electrolytes; see Figure 6. In these cases, the force in the bulk is always more repulsive than that at the interface. For 3:1 electrolyte, the force at intermediate



DOI: 10.1021/acs.jpcb.5b10105
J. Phys. Chem. B 2016, 120, 5817−5822

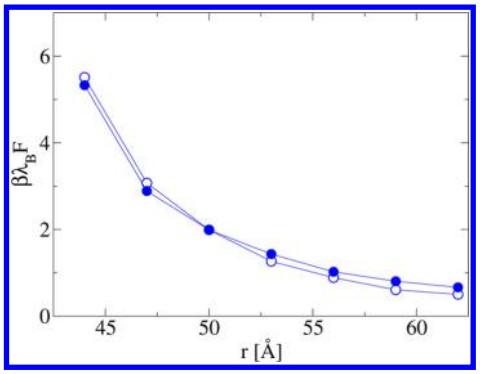


**Figure 4.** Force between two colloids. Empty symbols represent MC data for colloids in the bulk, while full ones, for colloids trapped at the air−water interface. The data is for salt at 75 mM ($\kappa$ = 0.09 Å$^{-1}$). The lines are guides to the eyes. Image charges are not considered.

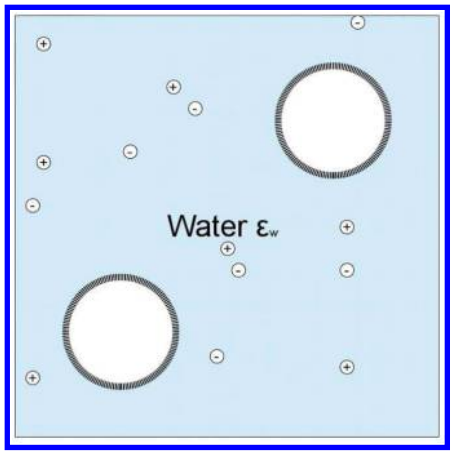


**Figure 5.** Two colloidal particles with charge $Z_{bulk}$ inside bulk electrolyte.

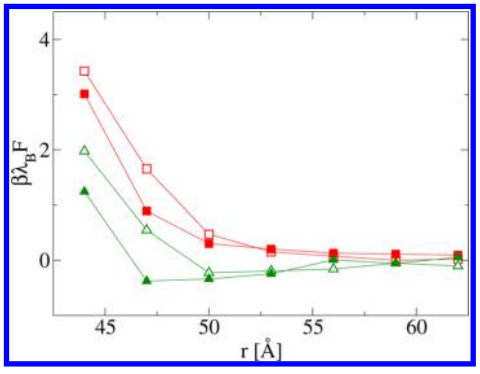


**Figure 6.** Force between two colloidal particles. Empty symbols represent the data for colloids in the bulk, while full ones, for colloidal particles trapped at the water−air interface. Squares are for 2:1 electrolyte, while triangles are for 3:1 electrolyte. The salt concentration is 75 mM, in both cases. The lines are guides to the eyes. Image charges are not included.

separation between the colloidal particles becomes attractive (negative). Attraction also appears in the bulk suspensions but is significantly weaker than at the interface.

We next explore the effect of the dielectric discontinuity across the interface on the interaction between trapped colloidal particles. In Figure 7, we show a comparison between the forces when the image charges are taken into account and when they are neglected. The induced charge at the air−water

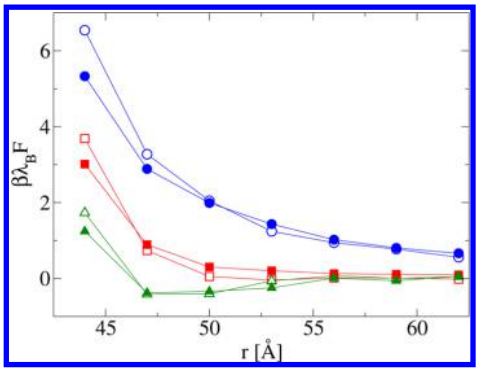


**Figure 7.** Comparison between the interaction force between two colloidal particles trapped at the air−water interface, calculated with and without image charges. The full symbols represent simulations without image charges, while empty symbols represent simulations with image charges. Circles, squares, and triangles are data for salts with monovalent, divalent, and trivalent counterions at 75 mM, respectively. The lines are guides to the eyes.

interface does not seem to affect significantly the interaction between the colloidal particles, except at very short separations.

## CONCLUSIONS

We studied the interaction force between colloidal particles trapped at an air−water interface. The high electrostatic free energy penalty of exposing charged groups to the low dielectric environment prevents ionization of these groups inside either air or oil. Therefore, only the surface groups which are hydrated will be ionized. For these groups, ionization is favored by the entropic free energy gain of counterion release, while the enthalpic electrostatic free energy penalty is lowered by screening of the exposed surface charge groups by the dipole moments of the surrounding water molecules. In view of this, we have idealized the interface-trapped colloidal particles as hard-spheres with the hemisphere exposed to water carrying a uniform surface charge and the other hemisphere remaining charge neutral. We found that the interface bound colloidal particles in 1:1 electrolyte interact with a force which is almost identical to the force between bulk colloids of the same total charge. The far-field weak dipole−dipole-like interaction cannot be seen in our simulations. This is consistent with a theoretical argument[11] that the crossover to dipole−dipole-like interaction will occur only at separations larger than $r \approx 9/\kappa$. At these distances, the interaction is so weak that it is beyond the statistical uncertainty of our simulations. The equality between bulk and surface forces breaks down for colloids in 2:1 and 3:1 electrolytes, for which the bulk interaction is always more repulsive than at the interface. Finally, we have explored the effect of dielectric discontinuity across the interface on the intercolloidal interaction. For all the cases studied, we have found only a small effect of image charges at very short separations between the colloidal particles. We hope that the work will provide a further stimulus to the development of analytical methods for studying colloidal particles trapped at dielectric interfaces between polar and nonpolar mediums.

## AUTHOR INFORMATION

### Corresponding Author

*E-mail: levin@if.ufrgs.br.

### Notes

The authors declare no competing financial interest.



DOI: 10.1021/acs.jpcb.5b10105
J. Phys. Chem. B 2016, 120, 5817−5822

## ■ ACKNOWLEDGMENTS

This work was partially supported by the CNPq, INCT-FCx, and by the US-AFOSR under grant FA9550-12-1-0438.

## ■ REFERENCES

(1) Hurd, A. J. The Electrostatic Interaction between Interfacial Colloidal Particles. *J. Phys. A: Math. Gen.* **1985**, *18*, L1055−L1060.
(2) Dinsmore, A. D.; Hsu, M. F.; Nikolaides, M. G.; Márquez, M.; Bausch, A. R.; Weitz, D. A. Colloidosomes: Selectively Permeable Capsules Composed of Colloidal Particles. *Science* **2002**, *298*, 1006−1009.
(3) Foret, L.; Würger, A. Electric-Field Induced Capillary Interaction of Charged Particles at a Polar Interface. *Phys. Rev. Lett.* **2004**, *92*, 058302−058305.
(4) Oettel, M.; Domínguez, A.; Dietrich, S. Effective Capillary Interaction of Spherical Particles at Fluid Interfaces. *Phys. Rev. E* **2005**, *71*, 051401−0514016.
(5) Oettel, M.; Domínguez, A.; Dietrich, S. Attractions Between Charged Colloids at Water Interfaces. *J. Phys.: Condens. Matter* **2005**, *17*, L337−L342.
(6) Würger, A.; Foret, L. Capillary Attraction of Colloidal Particles at an Aqueous Interface. *J. Phys. Chem. B* **2005**, *109*, 16435−16438.
(7) Loudet, J. C.; Alsayed, A. M.; Zhang, J.; Yodh, A. G. Capillary Interactions between Anisotropic Colloidal Particles. *Phys. Rev. Lett.* **2005**, *94*, 018301−018304.
(8) Gómez-Guzmán, O.; Ruiz-García, J. Attractive Interactions between Like-Charged Colloidal Particles at the Air/Water Interface. *J. Colloid Interface Sci.* **2005**, *291*, 1−6.
(9) Chen, W.; Tan, S.; Ng, T.; Ford, W. T.; Tong, P. Long-Ranged Attraction between Charged Polystyrene Spheres at Aqueous Interfaces. *Phys. Rev. Lett.* **2005**, *95*, 218301−218304.
(10) Chen, W.; Tan, S.; Huang, Z.; Ng, T.; Ford, W. T.; Tong, P. Measured Long-Ranged Attractive Interaction between Charged Polystyrene Latex Spheres at a Water-Air Interface. *Phys. Rev. E* **2006**, *74*, 021406−021419.
(11) Domínguez, A.; Oettel, M.; Dietrich, S. Theory of Capillary-Induced Interactions beyond the Superposition Approximation. *J. Chem. Phys.* **2007**, *127*, 204706−204722.
(12) Domínguez, A.; Oettel, M.; Dietrich, S. Force Balance of Particles Trapped at Fluid Interfaces. *J. Chem. Phys.* **2008**, *128*, 114904−114915.
(13) Frydel, D.; Oettel, M. Charged Particles at Fluid Interfaces as a Probe Into Structural Details of a Double Layer. *Phys. Chem. Chem. Phys.* **2011**, *13*, 4109−4118.
(14) Chen, Q.; Bae, S. C.; Granick, S. Directed Self-Assembly of a Colloidal Kagome Lattice. *Nature* **2011**, *469*, 381−384.
(15) Majee, A.; Bier, M.; Dietrich, S. Electrostatic Interaction between Colloidal Particles Trapped at an Electrolyte Interface. *J. Chem. Phys.* **2014**, *140*, 164906−164910.
(16) Pieranski, J. Two-Dimensional Interfacial Colloidal Crystals. *Phys. Rev. Lett.* **1980**, *45*, 569−573.
(17) Aveyard, R.; Clint, J. H.; Nees, D.; Paunov, V. N. Compression and Structure of Monolayers of Charged Latex Particles at Air/Water and Octane/Water Interfaces. *Langmuir* **2000**, *16*, 1969−1979.
(18) Aveyard, R.; Binks, B. P.; Clint, J. H.; Fletcher, P. D. I.; Horozov, T. S.; Neumann, B.; Paunov, V. N.; Annesley, J.; Botchway, S. W.; Need, D.; et al. Measurement of Long-Range Repulsive Forces between Charged Particles at an Oil-Water Interface. *Phys. Rev. Lett.* **2002**, *88*, 246102−246105.
(19) Park, B. J.; Pantina, J. P.; Furst, E. M.; Oettel, M.; Reynaert, S.; Vermant, J. Direct Measurements of the Effects of Salt and Surfactant on Interaction Forces between Colloidal Particles at Water-Oil Interfaces. *Langmuir* **2008**, *24*, 1686−1694.
(20) Oettel, M.; Dietrich, S. Colloidal Interactions at Fluid Interfaces. *Langmuir* **2008**, *24*, 1425−1441.
(21) Domínguez, A.; Frydel, D.; Oettel, M. Multipole Expansion of the Electrostatic Interaction between Charged Colloids at Interfaces. *Phys. Rev. E* **2008**, *77*, 020401−020404.
(22) Levin, Y. Electrostatic Correlations: from Plasma to Biology. *Rep. Prog. Phys.* **2002**, *65*, 1577−1632.
(23) Frenkel, D.; Smit, B. *Understanding Molecular Simulation - From Algorithms to Applications*; Academic Press: San Diego, CA, 2002; pp 291−306.
(24) De Leeuw, S. W.; Perram, J. W. Electrostatic Lattice Sums for Semi-Infinite Lattices. *Mol. Phys.* **1979**, *37*, 1313−1322.
(25) Spohr, E. Effect of Electrostatic Boundary Conditions and System Size on the Interfacial Properties of Water and Aqueous Solutions. *J. Chem. Phys.* **1997**, *107*, 6342−6348.
(26) Harris, F. E. Ewald Summations in Systems With Two-Dimensional Periodicity. *Int. J. Quantum Chem.* **1998**, *68*, 385−404.
(27) Hautman, J.; Halley, J. W.; Rhee, Y. J. Molecular Dynamics Simulation of Water beween Two Ideal Classical Metal Walls. *J. Chem. Phys.* **1989**, *91*, 467−472.
(28) Rhee, Y. J.; Halley, J. W.; Hautman, J.; Rahman, A. Ewald Methods in Molecular Dynamics for Systems of Finite Extent in One of Three Dimensions. *Phys. Rev. B: Condens. Matter Mater. Phys.* **1989**, *40*, 36−42.
(29) Hautman, J.; Klein, M. L. An Ewald Summation Method for Planar Surfaces and Interfaces. *Mol. Phys.* **1992**, *75*, 379−395.
(30) Aloisi, G.; Foresti, M. L.; Guidelli, R.; Barnes, P. A Monte Carlo Simulation of Water Molecules Near a Charged Wall. *J. Chem. Phys.* **1989**, *91*, 5592−5596.
(31) Liem, S. Y.; Clarke, J. H. R. Calculation of Coulomb Interactions in Two-Dimensionally Periodic Systems. *Mol. Phys.* **1997**, *92*, 19−25.
(32) Widmann, A. H.; Adolf, D. B. A Comparison of Ewald Summation Techniques for Planar Surfaces. *Comput. Phys. Commun.* **1997**, *107*, 167−186.
(33) Shelley, J. C. Boundary Condition Effects in Simulations of Water Confined Between Planar Walls. *Mol. Phys.* **1996**, *88*, 385−398.
(34) Smith, E. R. Electrostatic Energy in Ionic Crystals. *Proc. R. Soc. London, Ser. A* **1981**, *375*, 475−505.
(35) Yeh, I.; Berkowitz, M. L. Ewald Summation for Systems with Slab Geometry. *J. Chem. Phys.* **1999**, *111*, 3155−3162.
(36) Boresch, S.; Steinhauser, O. Presumed versus Real Artifacts of the Ewald Summation Technique: The Importance of Bielectric Boundary Conditions. *Ber. Bunsenges. Phys. Chem.* **1997**, *101*, 1019−1029.
(37) Bogusz, S.; Cheatham, T. E., III; Brooks, B. R. Removal of Pressure and Free Energy Artifacts in Charged Periodic Systems via Net Charge Corrections to the Ewald Potential. *J. Chem. Phys.* **1998**, *108*, 7070−7084.
(38) Roberts, J. E.; Schnitker, J. How The Unit Cell Surface Charge Distribution Affects the Energetics of Ion-Solvent Interactions in Simulations. *J. Chem. Phys.* **1994**, *101*, 5024−5031.
(39) Roberts, J. E.; Schnitker, J. Boundary Conditions in Simulations of Aqueous Ionic Solutions: A Systematic Study. *J. Phys. Chem.* **1995**, *99*, 1322−1331.
(40) dos Santos, A. P.; Levin, Y. *Electrostatics of Soft and Disordered Matter*; CRC Press: Boca Raton, FL, 2014; Chapter 14.
(41) dos Santos, A. P.; Levin, Y. Electrolytes between Dielectric Charged Surfaces: Simulations and Theory. *J. Chem. Phys.* **2015**, *142*, 194104−194110.
(42) Wu, J. Z.; Bratko, D.; Blanch, H. W.; Prausnitz, J. M. Monte Carlo Simulation for the Potential of Mean Force between Ionic Colloids in Solutions of Asymmetric Salts. *J. Chem. Phys.* **1999**, *111*, 7084−7093.
(43) Colla, T. E.; dos Santos, A. P.; Levin, Y. Equation of State of Charged Colloidal Suspensions and its Dependence on the Thermodynamic Route. *J. Chem. Phys.* **2012**, *136*, 194103−194109.
(44) dos Santos, A. P.; Bakhshandeh, A.; Levin, Y. Effects of the Dielectric Discontinuity on the Counterion Distribution in a Colloidal Suspension. *J. Chem. Phys.* **2011**, *135*, 044124−044128.
(45) Bakhshandeh, A.; dos Santos, A. P.; Levin, Y. Weak and Strong Coupling Theories for Polarizable Colloids and Nanoparticles. *Phys. Rev. Lett.* **2011**, *107*, 107801−107805.



DOI: 10.1021/acs.jpcb.5b10105
*J. Phys. Chem. B* 2016, 120, 5817−5822

(46) Alexander, S.; Chaikin, P. M.; Grant, P.; Morales, G. J.; Pincus, P. Charge Renormalization, Osmotic Pressure, and Bulk Modulus of Colloidal Crystals: Theory. *J. Chem. Phys.* **1984**, *80*, 5776−5781.
(47) dos Santos, A. P.; Diehl, A.; Levin, Y. Electrostatic Correlations in Colloidal Suspensions: Density Profiles and Effective Charges beyond the Poisson-Boltzmann Theory. *J. Chem. Phys.* **2009**, *130*, 124110−124113.



DOI: 10.1021/acs.jpcb.5b10105
*J. Phys. Chem. B* 2016, 120, 5817−5822